Robust Adaptive Local Polynomial Fourier Transform

Igor Djurović

Abstract— **A robust form of the local polynomial Fourier transform (LPFT) is introduced. This transform can produce a highly concentrated time-frequency (TF) representation for signals embedded in an impulse noise. Calculation of the adaptive parameter in the proposed transform is based on the concentration measure. A modified form, calculated as a weighted sum of the robust LPFT, is proposed for multicomponent signals.**

I. Introduction

In many practical applications signals are disturbed by an impulse noise. It could be caused by atmospheric or human-made disturbances. The short-time Fourier transform (STFT), as well as other standard TF representations, behave poorly in impulse noise environments. The robust STFT has been introduced recently to overcome this drawback [1]. It is slightly worse than the standard STFT for a Gaussian noise environment, while it is significantly better than its standard counterpart for an impulse noise environment. Unfortunately, for nonstationary signals both STFT forms have low concentration and small TF resolution [2]. The robust LPFT is proposed in this letter to produce highly concentrated TF representation for signals embedded in an impulse noise. This transform depends on the chirp-rate parameter. Adaptive determination of the chirp-rate parameter is done based on the concentration measure. The adaptive weighted sum of the LPFTs is proposed for the TF analysis of multicomponent signals.

The paper is organized as follows. The robust STFT is reviewed in Section II, while the adaptive robust LPFT is introduced in Section III. Modification of the proposed transform for multicomponent signals is presented in Section IV. Numerical examples are given in Section V.

IEEE Signal Processing Letters, Vol. 11, No.2, Feb. 2004

II. Robust STFT

The STFT forms, for a signal $x(t)$, can be defined by using the following minimization problem:

$$STFT(t,\omega) = \arg\left\{\min_m J(t,\omega;m)\right\}, \quad (1)$$

$$J(t,\omega;m) = \sum_{n=-N/2}^{N/2-1} F(e(t,\omega,n;m)), \quad (2)$$

where $F(e)$ is the loss function, while the error function is given as:

$$e(t,\omega,n;m) = x(t+nT)\exp(-j\omega nT) - m, \quad (3)$$

where T is the sampling rate. Minimization problem (1)-(3) produces the standard STFT, robust M-STFT [1], and robust STFT in the marginal-median form [3], for loss functions $F(e) = |e|^2$, $F(e) = |e|$, and $F(e) = |\operatorname{Re}(e)| + |\operatorname{Im}(e)|$, respectively:

$$STFT_S(t,\omega) = \frac{1}{N}\sum_{n=-N/2}^{N/2-1} x(t+nT)\exp(-j\omega nT)$$
$$= \operatorname{mean}\{x(t+nT)\exp(-j\omega nT) \quad |n \in [-N/2, N/2)\}, \quad (4)$$

$$STFT_{R1}(t,\omega) = \frac{1}{\sum_{n=0}^{N-1}|e_1(t,\omega,n)|^{-1}} \times \sum_{n=-N/2}^{N/2-1} \frac{x(t+nT)\exp(-j\omega nT)}{|e_1(t,\omega,n)|}, \quad (5)$$

$$STFT_{R2}(t,\omega) = \operatorname{median}\{\operatorname{Re}\{x(t+nT)\exp(-j\omega nT)\}|$$

$$n \in [-N/2, N/2)\}+$$

$$j\text{median}\{\text{Im}\{x(t+nT)\exp(-j\omega nT)\}|$$

$$n \in [-N/2, N/2)\}. \quad (6)$$

Expression (5) is an implicit definition of the $STFT_{R1}(t,\omega)$, since $e_1(t,\omega,n)$ is a function of $STFT_{R1}(t,\omega)$:

$$e_1(t,\omega,n) =$$

$$x(t+nT)\exp(-j\omega nT) - STFT_{R1}(t,\omega). \quad (7)$$

Note that application of the loss function $F(e) = |e|$, in order to produce solutions robust to the impulse noise influence, is common in signal processing (see [1] and references therein). An iterative procedure is required for solving (5), while sorting procedures are necessary for calculation of $STFT_{R2}(t,\omega)$ [1]. These procedures should be employed for each point in the TF plane. Sorting procedures are faster than the iterative ones. In addition, sorting procedures avoid the convergence problem. Both robust STFT forms (5) and (6) have similar performances. They are slightly worse in the Gaussian environment, and significantly better in the impulse noise environment, than the standard STFT [3]. Unfortunately, they produce weak TF resolution and TF concentration for nonstationary signals. This is the reason for introducing the robust LPFT in the following section.

III. Robust LPFT

The LPFT can be defined as [4]:

$$LPFT(t,\omega,\alpha_0,...,\alpha_{M-2}) =$$

$$\frac{1}{N}\sum_{n=-N/2}^{N/2-1} x(t+nT)\times$$

$$\exp\left(-j\omega nT - j\sum_{m=2}^{M}\alpha_{m-2}\frac{(nT)^m}{m!}\right). \quad (8)$$

In order to decrease calculation burden, the LPFT for $M = 2$ will be considered:

$$LPFT_{\alpha(t)}(t,\omega) = \frac{1}{N}\sum_{n=-N/2}^{N/2-1} x(t+nT)\times$$

$$\exp\left(-j\omega nT - j\alpha(t)(nT)^2/2\right), \quad (9)$$

where $\alpha(t)$ is time-varying chirp parameter. The LPFT can be better concentrated than the STFT for signals with nonstationary spectral content. As an example, consider a linear FM signal:

$$x(t) = A\exp(jat^2/2 + jbt). \quad (10)$$

Approximative expression for the STFT of the linear FM signal is derived in [6]:

$$|STFT_S(t,\omega)| \approx A\sqrt{\frac{2\pi}{a}}p\left(\frac{\omega - at - b}{a}\right), \quad (11)$$

where $p(t)$ is the rectangular window function, $p(t) = 1$ for $|t| \leq NT/2$, and $p(t) = 0$ otherwise. It can be seen that concentration of the TF component decreases as parameter a increases. In addition, the TF resolution (possibility for separation of close signal components) decreases. The LPFT of the linear FM signal is given as:

$$|LPFT_{\alpha(t)}(t,\omega)| \approx A\sqrt{\frac{2\pi}{|\alpha(t)-a|}}\times$$

$$\left|\exp(j\left(\omega - at - b\right)^2/4(\alpha(t)-a)) *_\omega P(\omega)\right|, \quad (12)$$

where $*_\omega$ is convolution in the frequency domain, while $P(\omega)$ is Fourier transform of the window function $p(t)$. The LPFT is ideally concentrated along the instantaneous frequency (IF), $\omega(t) = at + b$, for $\alpha(t) = a$. Similarly, it can be proved that for a nonlinear FM signal, $x(t) = A\exp(j\phi(t))$, the highest concentration can be achieved by those LPFT with the chirp-rate parameter close to the second derivative of the signal phase, $\alpha(t) \approx \phi''(t)$. The LPFT can alternatively be written as:

$$LPFT_{\alpha(t)}(t,\omega) = STFT_S(t,\omega) *_\omega$$

$$FT\left\{\exp\left(-j\alpha(t)(nT)^2/2\right)\right\}, \quad (13)$$

where $FT\{\}$ denotes the Fourier transform operator. By analogy, the robust LPFT can be defined based on the robust STFT as:

$$rLPFT_{\alpha(t)}(t,\omega) = STFT_R(t,\omega) *_\omega$$

$$FT\left\{\exp\left(-j\alpha(t)(nT)^2/2\right)\right\}, \quad (14)$$

where $STFT_R(t,\omega)$ can be either of the robust STFT forms (5), (6). Alternatively, it can be defined as:

$$rLPFT_{\alpha(t)}(t,\omega) = \frac{1}{N}\sum_{n=-N/2}^{N/2-1} IFT_{\omega\to nT}\{STFT_R(t,\omega)\}\times \exp\left(-j\omega nT - j\alpha(t)(nT)^2/2\right), \quad (15)$$

where:

$$IFT_{\omega\to nT}\{STFT_R(t,\omega)\} = \frac{N}{2\pi}\int_{-\pi}^{\pi} STFT_R(t,\omega)e^{j\omega nT}d\omega. \quad (16)$$

Expression $IFT_{\omega\to nT}\{STFT_R(t,\omega)\}$ can be considered as an estimate of the noise-free signal samples in the range $[t-NT/2, t+NT/2)$. Calculation of the robust LPFT requires realization of the robust STFT by sorting or by iterative procedures and implementation of two FFT algorithms for evaluation of (15) and (16).

The remaining problem is how to determine the unknown chirp-rate $\alpha(t)$. It can be seen from (12) that the concentration of the standard LPFT can be connected directly to the chirp-rate value. Obviously, the same situation holds for the robust LPFT. Then the adaptive TF representation can be calculated by using the chirp-rate which produces the highest concentration in the TF plane. An overview of concentration measures used in the TF analysis can be found in [5] and references therein. The concentration measure proposed in [7] will be used here. The adaptive form of (14) is given as:

$$AFT(t,\omega) = rLPFT_{\hat{\alpha}(t)}(t,\omega), \quad (17)$$

$$\hat{\alpha}(t) = \arg\left\{\max_{\alpha\in\Lambda} H(\alpha,t)\right\}, \quad (18)$$

where Λ is a set of considered chirp-rate parameter values, while $H(\alpha,t)$ is a concentration measure [7]:

$$H(\alpha,t) = \frac{\int_{-\infty}^{\infty}|rLPFT_\alpha(t,\omega)|^2 d\omega}{\left(\int_{-\infty}^{\infty}|rLPFT_\alpha(t,\omega)|d\omega\right)^{3/2}}. \quad (19)$$

Note that this particular concentration measure achieves very sharp maximum for α close to the second derivative of the signal phase [7]. It is a very favorable property for signals embedded in a high noise environment.

The proposed transform, $AFT(t,\omega)$, draws good properties from both the robust STFT (robustness to the impulse noise influence) and the standard LPFT (high concentration along the IF for properly selected chirp-rate parameter).

IV. Adaptive Weighted Robust LPFT

For multicomponent signals, the previously defined adaptive TF representation would be adjusted on dominant signal component, i.e., component of the highest magnitude. However, in that case, other components will not be represented properly. In order to overcome this drawback, we propose the following form of the adaptive robust LPFT [8]:

$$AFT'(t,\omega) = \sum_{\alpha\in\Lambda} g(\alpha,t)rLPFT_\alpha(t,\omega), \quad (20)$$

where $g(\alpha,t)$ are weighted coefficients. Strategy for selecting weighted coefficients depends on the considered signal type. If a signal has numerous components but with similar chirp rates, then it is appropriate to select $g(\hat{\alpha}(t),t) = 1$, where $\hat{\alpha}(t)$ is the element from Λ producing the highest concentration in the considered instant (18), and $g(\alpha,t) = 0$ for $\alpha \neq \hat{\alpha}(t)$. In this way we ensure that all components are concentrated reasonably. This is similar to the monocomponent signals case and it can be used in speech processing, combustion knock analysis, etc. For signals with numerous components but with only several chirp-rates, the following procedure could be used: (a) Set $H^{(0)}(\alpha,t) = H(\alpha,t)$, $i = 0$. (b) Determine $\hat{\alpha}^{(i)}(t) = \arg\max_\alpha H^{(i)}(\alpha,t)$, $i = i+1$. (c) Set $g(\hat{\alpha}^{(i)}(t),t) = 1$. (d) Set $H^{(i)}(\alpha,t) = H^{(i-1)}(\alpha,t)$ for $\alpha \notin [\hat{\alpha}^{(i)}(t) - \Delta, \hat{\alpha}^{(i)}(t)+\Delta]$, $H^{(i)}(\alpha,t) = 0$ elsewhere. Steps (b)-(d) should be repeated for each chirp-rate producing high concentration measure. Procedure should be stopped if there are no more α producing high values of $H^{(i)}(\alpha,t)$. This procedure can be used in analysis of vibrations,

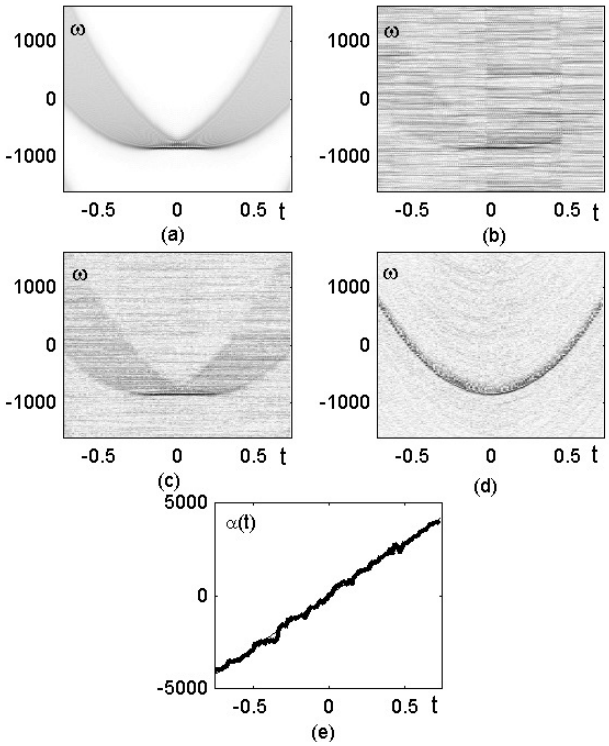

Fig. 1. TF representations of signal embedded in impulse noise: (a) $STFT_S(t,\omega)$ of non-noisy signal; (b) $STFT_S(t,\omega)$; (c) $STFT_{R2}(t,\omega)$; (d) $AFT(t,\omega)$; (e) $\hat{\alpha}(t)$.

frequency coded signals, etc. Signals with numerous distinct chirp rates require more sophisticated procedures outside of the scope of this paper.

V. Numerical Examples

Example 1. Consider a signal:

$$f(t) = \exp(j\phi(t)) = \exp(j300\pi t^3 - j275\pi t), \tag{21}$$

sampled with $T = 1/512$ within $t \in [-3/4, 3/4]$. The standard STFT of non-noisy signal $f(t)$ is shown in Fig.1a. The signal is corrupted by a high amount of the impulse noise, $x(t) = f(t) + \nu(t)$, $\nu(t) = 0.5(\nu_1^3(t) + j\nu_2^3(t))$, where $\nu_i(t)$, $i = 1, 2$, are mutually independent Gaussian noises with zero mean and unitary variance, $E\{\nu_i(t)\nu_j(t)\} = \delta(i-j)$. The standard STFT of the noisy signal is depicted in Fig.1b. Signal component cannot be observed from Fig.1b. The robust STFT given by (6) is presented in Fig.1c. The signal component can easily be seen from Fig.1c, but it is spread over the TF plane, especially in the region with rapid variation of the IF, $\omega(t) = \phi'(t)$. The adaptive robust LPFT, calculated by using $STFT_{R2}(t,\omega)$, is depicted in Fig.1d, while the adaptive chirp parameter $\hat{\alpha}(t)$ is given in Fig.1e. The chirp-rate parameter is considered within the range $\alpha \in [-2048\pi, 2048\pi]$ with 128 equidistant values. It can be concluded from these figures that the adaptive robust LPFT is highly concentrated along the IF, while the adaptive chirp-rate parameter is approximately equal to the IF derivative, $\hat{\alpha}(t) \approx \omega'(t) = \phi''(t) = 1800\pi t$.

Signal (21) embedded in the white complex Gaussian noise $\nu(t) = 0.75(\nu_1(t) + j\nu_2(t))$ is considered in order to prove that the proposed transform produces only slightly worse results than the standard LPFT in the Gaussian noise environment. The standard and robust STFT are depicted in Figs.2a,b, while the corresponding LPFTs are given in Figs.2c,d. Chirp-

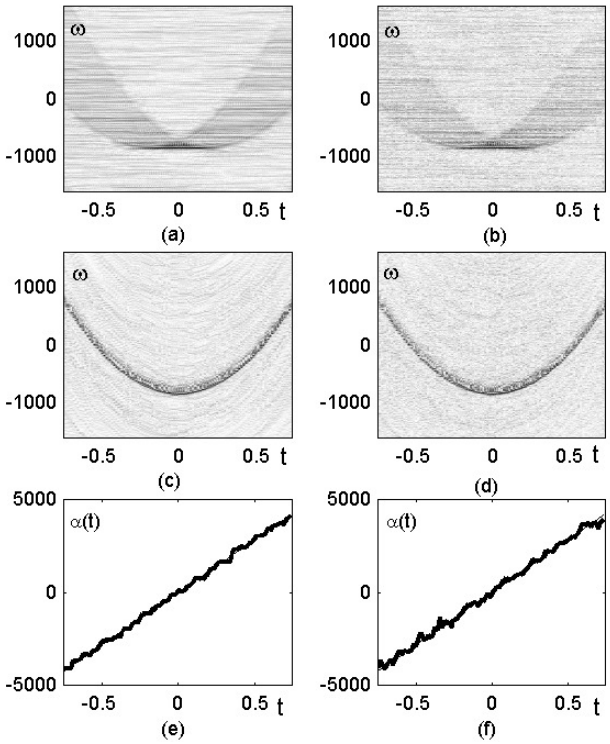

Fig. 2. TF representations of signal embedded in Gaussian noise: (a) $STFT_S(t,\omega)$; (b) $STFT_{R2}(t,\omega)$; (c) $AFT(t,\omega)$ calculated by the standard LPFT; (d) $AFT(t,\omega)$ calculated by the robust LPFT; (e) Chirp-rate estimation by using the standard LPFT; (f) Chirp-rate estimation by using the robust LPFT.

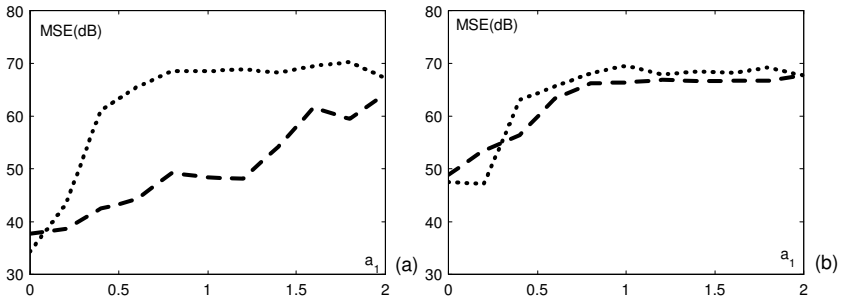

Fig. 3. MSE of the chirp-rate estimation: (a) Impulse noise environment; (b) Mixture of Gaussian and impulse noise. Dashed line - adaptive robust LPFT; Dotted line - adaptive standard LPFT.

rate estimates obtained by using the concentration measure are shown in the third row of Fig.2. It can be seen that the chirp-rate estimate based on the robust LPFT is only slightly worse than the corresponding one produced by the standard LPFT form.

Performance of the proposed transform with respect to the chirp-rate estimation is examined for signal (21) embedded in a mixture of the impulse and Gaussian noise:

$$\nu(t) = a_1(\nu_1^3(t) + j\nu_2^3(t)) + a_2(\nu_1(t) + j\nu_2(t)), \tag{22}$$

where $\nu_i(t)$, $i = 1,2,3,4$, are mutually independent white Gaussian noises with unitary

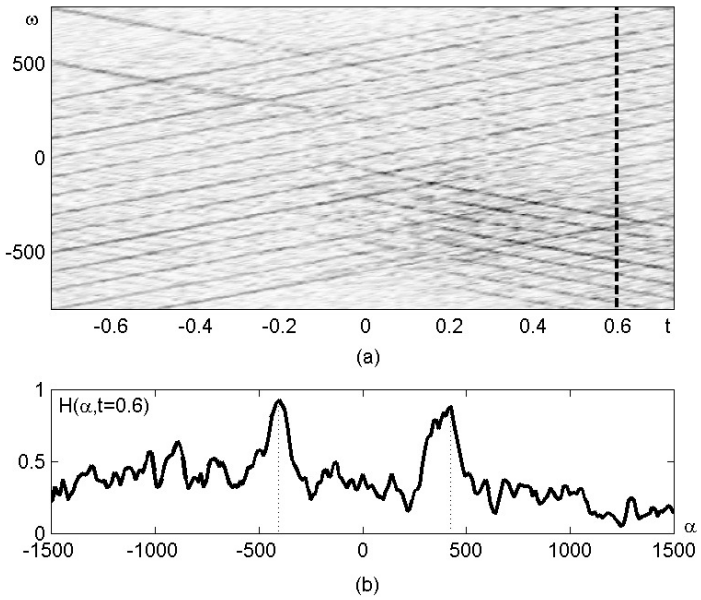

Fig. 4. Multicomponent signals: (a) $AFT'(t,\omega)$ (instant $t = 0.6$ is marked with dashed line); (b) $H(\alpha, t)$ for $t = 0.6$.

variance $E\{\nu_i(t)\nu_j(t)\} = \delta(i-j)$. We considered two experiments: (a) Impulse noise ($a_2 = 0$); (b) Mixture of the impulse noise with a high amount of the Gaussian noise ($a_2 = 1$). In both experiments various amounts of impulse noise are considered, $a_1 \in [0, 2]$. In order to produce precise a comparison, the set of considered parameters α has been extended to 512 different values. For each noise amount, a set of 100 trials is considered. The MSE of the chirp-rate estimation is depicted in Fig.3. It can be seen that the proposed adaptive robust LPFT significantly outperforms the standard LPFT based realization in the impulse noise environment. The proposed transform is better than the standard one for the mixture, except for a very small amount of the impulse noise.

Example 2. Consider a multicomponent signal:

$$f(t) = f_1(t) + f_2(t)u(t) + f_3(t)u(-t) \quad (23)$$

where $f_1(t) = \sum_{k=-6}^{6} \exp(j64\pi t^2 + jk32\pi t + j\varphi_k)$, $f_2(t) = \sum_{k=0}^{8} \exp(-j64\pi t^2 - jk24\pi t + j\varphi'_k)$, $f_3(t) = \sum_{k=0}^{1} \exp(-j64\pi t^2 + j64\pi t + jk92\pi t + j\varphi''_k)$, $u(t) = 1$ for $t \geq 0$ and $u(t) = 0$ elsewhere. Phases φ_k, φ'_k and φ''_k are selected randomly within $[0, 2\pi)$. Impulse noise environment is modeled as $\nu(t) = 0.5(\nu_1^3(t) + j\nu_2^3(t))$. Signal has 22 components for $t \geq 0$ (13 with increasing frequencies and 9 with decreasing), and 15 components for $t < 0$ (13 with increasing frequencies and 2 with decreasing), but only two chirp-rates in each instant. The adaptive weighted robust LPFT is depicted in Fig.4a. All signal components can be easily seen from this figure. Note that other TF representations considered in this paper cannot be used to produce such accuracy. Concentration measure $H(\alpha, t)$ in $t = 0.6$ is given in Fig.4b, where chirp-rates corresponding to selected robust LPFTs in the sum (20) are marked with dotted lines.

VI. Conclusion

Two forms of the adaptive robust LPFT are proposed in this letter. Adaptive parameter $\alpha(t)$ in the first, and weighted coefficients in the second form, are determined by using the concentration measure. Obtained TF representations are highly concentrated along the IF. They are robust to the impulse noise influ-

ence.

Acknowledgment

This work is supported by the Volkswagen Stiftung, Federal Republic of Germany. Part of this research has been done at the Kyoto Institute of Technology, supported by Postdoctoral Fellowship for Foreign Researchers of Japan Society for the Promotion of Science.

References

[1] V. Katkovnik, "Robust M-periodogram," *IEEE Trans. Sig. Proc.*, Vol. 46, No.11, Nov. 1998, pp. 3104-3109.

[2] F. Hlawatsch and G. F. Boudreaux-Bartels, "Linear and quadratic time-frequency signal representations," *IEEE Sig. Proc. Mag.*, Vol. 9, No.4, Apr. 1992, pp. 21-67.

[3] I. Djurović, V. Katkovnik and LJ. Stanković, "Median filter based realizations of the robust time-frequency distributions," *Sig. Proc.*, Vol. 81, No.7, July 2001, pp. 1771-1776.

[4] V. Katkovnik, "A new form of the Fourier transform for time-frequency estimation," *Sig. Proc.*, Vol. 47, No.2, 1995, pp. 187-200.

[5] R. G. Baraniuk, P. Flandrin, A. J. E. M. Janssen and O. J. J. Michel, "Measuring time-frequency information content using the Renyi entropies," *IEEE Trans. Inf. Th.*, Vol. 47, No.4, May 2001, pp. 1391-1409.

[6] LJ. Stanković: "The auto-term representation by the reduced interference distributions; The procedure for a kernel design," *IEEE Trans. Sig. Proc.*, Vol. 44, No. 6, June 1996, pp. 1557-1564.

[7] F. Zhang, Y.-Q. Chen and G. Bi, "Adaptive harmonic fractional Fourier transform," *IEEE Sig. Proc. Let.*, Vol. 6, No.11, Nov. 1999, pp. 281-283.

[8] M. Daković, I. Djurović and LJ. Stanković, "Adaptive local polynomial Fourier transform," *EUSIPCO 2002*, Toulouse, France, Sep. 2002, Vol.II, pp. 603-606.